13th World Conference on Earthquake Engineering
Vancouver, B.C., Canada
August 1-6, 2004
Paper No. 200

EVALUATION OF LIQUEFACTION POTENTIAL BY FREQUENCY-DEPENDENT EQUIVALENT LINEARIZED TECHNIQUE

Atsushi YASHIMA[1], Masata SUGITO[2] and Hisaki OKADA3[1]

SUMMARY

A conventional equivalent linearized technique (SHAKE), a frequency-dependent equivalent linearized technique (FDEL) and an effective stress based FEM technique were used to evaluate the liquefaction potential for three typical ground under different input motions. The liquefaction potentials obtained from SHAKE and FDEL were compared with those obtained from the effective stress based FEM. It is found from the comparative studies that FDEL possessed higher reliability for evaluating liquefaction potential for soft ground than SHAKE. It was, however, found that FDEL predicted much higher liquefaction potentials under a very large input motions and lower liquefaction potentials for the ground with several stiff strata than the effective stress based FEM.

INTRODUCTION

In order to prevent the severe damage due to liquefaction, firstly we have to predict the liquefaction potential precisely for the site. Although it is possible, at present time, to analyze liquefaction process of ground due to earthquake at an acceptable accurate level by conducting an effective stress analysis with cyclic elasto-plastic or ealsto-viscoplastic constitutive models for sand and clay, the analytical procedure needs detailed parameters on soil properties, considerable time and cost. On the other hand, an equivalent linearized technique has been successfully used to analyze the ground response during earthquake because of its simplicity. Therefore we have to investigate the applicability and limitation of an equivalent linearized technique for predicting liquefaction potential.

In this study, a conventional equivalent linearized technique (SHAKE), a frequency-dependent equivalent linearized technique (FDEL) and an effective stress based FEM technique (LIQCA) are used to evaluate the liquefaction potential for three typical ground under three different input motions. In the finite element analysis, the liquefaction resistance factor is newly proposed by introducing the concept of liquefaction threshold. The liquefaction potentials obtained by SHAKE and FDEL are carefully compared with those obtained from the effective stress based FEM.

[1] Professor, Gifu University, Gifu, Japan, Email: yashima@cc.gifu-u.ac.jp
[2] Professor, Gifu University, Gifu, Japan, Email: sugito@cive.gifu-u.ac.jp
[3] Engineer, Tokyu Construction, Tokyo, Japan , Email: okada@hd.tokyu-cnst.co.jp

FLECUENCY-DEPENDENT EQUIVALENT LINEARIZED TECHNIQUE (FDEL)

An equivalent linearized method, in which the non-linear characteristics of shear modulus and damping factor of soil is equalized by an equivalent linear relations of the shear strain, has been applied commonly for seismic response analysis of ground. Computer programs based on this method, such as SHAKE (Schnabel et. Al. [1]) has been widely used. SHAKE is based on a multi-reflection theory and is suitable for the analysis of horizontally layered ground. It has been pointed out however, that the calculated responses of sediments did not agree with the observations in the case of strong ground vibration. In particular, the results of high frequency components are underestimated if compared with the observed records in soft layers.

In conventional equivalent linearized technique, if strain level is large, the equivalent shear modulus and damping factor will be regulated at the large strain level. In the case of soft soil, as a result, damping factor of high frequency component is estimated exceedingly large. Since the time history of a strain, in general, is strongly characterized by the frequency, the frequency-dependent equivalent stain is defined for evaluation of equivalent shear modulus and damping factor of soil in frequency domain (Sugito et. Al. [2]). This technique, which is named FDEL, successfully improved SHAKE on the analysis of horizontally layered soft ground.

Definition of frequency dependent equivalent strain

The shear modulus and damping factor of soils have been examined in a large amount of laboratory tests, regarding the shear strain magnitude and the confining pressure. They have been modeled as a function of shear strain. In the conventional equivalent linearized technique, which is called CVT in this paper, some percentage of peak shear strain is used to determine the shear modulus and damping factor according to these modeled functions on G-γ, h-γ relations. In the program SHAKE, one of the CVT, the equivalent mean shear strain, γ_e, is fixed as 65% of the maximum strain, $\gamma_{\max}$ **:** namely, $\gamma_e = 0.65\ \gamma_{max}$. The numerical calculations are carried out until the deviation of γ_e from that given in the former calculation converges to the expected level.

Generally the ground motion includes some spectral characteristics, and the contribution of the frequency contents to strain time history strongly depend on frequency. Since the strong spectral characteristic of shear strain amplitude are included in the seismic ground response, it may be derived that appropriate shear modulus and damping depending on the frequency characteristic could be used for equivalent linearized analysis. According to this assumption the frequency-dependent equivalent strain is proposed in the following equation:

$$\gamma_f(\omega) = C\gamma_{\max}\frac{F_\gamma(\omega)}{F_{\gamma_{\max}}} \tag{1}$$

where C = constant, γ_{max} = maximum shear strain, $F\gamma(\omega)$ = Fourier spectrum of shear strain, and $F\gamma_{\max}$ represents the maximum of $F\gamma(\omega)$. The definition of $\gamma_f(\omega)$ in the left side of equation (1) is described that the equivalent strain, which controls equivalent shear modulus and damping factor, is given in proportional to the spectral amplitude of shear strain in frequency domain. The constant C controls the level of equivalent strain uniformly along the frequency axis. The condition $F\gamma(\omega) / F\gamma_{\max} = 1.0$ and $C = 0.65$ gives the same condition as CVT. The technique proposed here is called FDEL (Frequency-Dependent Equivalent Linearized technique).

It is commonly known that the relationship between shear strain γ and shear modulus G, and the relationship between shear strain γ and damping factor h, can be given by Hardin-Drnevich model (Hardin

and Drnevich [3]) in the analysis by using equivalent linearized technique. If the frequency-dependent equivalent strain is incorporated into Hardin-Drnevich model, next equations can be obtained,

$$\frac{G(\omega)}{G_{\max}(\omega)} = \frac{1}{1+\gamma_f(\omega)/\gamma_r} \tag{2}$$

$$\frac{h(\omega)}{h_{\max}(\omega)} = \frac{\gamma_f(\omega)/\gamma_r}{1+\gamma_f(\omega)/\gamma_r} \tag{3}$$

where the reference strain γ_r ($\gamma_r = \tau_{\max}/G_{\max}$) is given at each soil, as shown in Figure 1. If it is assumed that Poisson's ratio ν is constant, the relationship between stress and strain under plane strain condition is described as follows,

$$(\sigma_x \quad \sigma_y \quad \tau)^T = D(\varepsilon_x \quad \varepsilon_y \quad \gamma)^T \tag{4}$$

$$D = \begin{pmatrix} \frac{2G^*(1-\nu)}{1-2\nu} & \frac{2\nu G^*}{1-2\nu} & 0 \\ \frac{2\nu G^*}{1-2\nu} & \frac{2G^*(1-\nu)}{1-2\nu} & 0 \\ 0 & 0 & G^* \end{pmatrix} \tag{5}$$

where G^* is complex rigidity as follows

$$G^* = G(\omega) + i2\omega h(\omega) \tag{6}$$

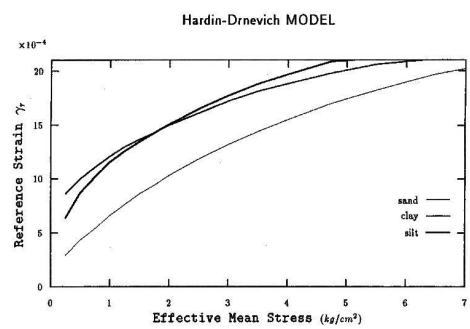

Figure 1. Reference Strain for each soil in Hardin-Drnevich Model

Definition of frequency dependent equivalent strain

The numerical calculations are carried out by using the equivalent shear modulus and damping factor at each layer, which are given by Equation (1). The equivalent strain for each frequency given by the equation is compared with the one given in the previous calculation. The iterative calculations are carried out until the error in the equivalent strain defined by the equation compared with the previous value, is converged to certain level. In FDEL, the convergence judgement is performed individually in three frequency regions such as, (a) low frequency region (1 Hz or lower), (b) middle frequency region (1 to 5 Hz), and (3) high frequency region (5 Hz or higher). The average of deviation in each frequency region is calculated, and the iterative procedures are continued until the deviation in each frequency region is converged into the given level. These divisions of the convergence judgement on the frequency axis are incorporated to consider the following ground motion characteristic.

1) low frequency region (lower than 1 Hz): low strain amplitude and long wave length [linear response region]
2) middle frequency region (from 1 to 5 Hz): large strain amplitude and large non-linear effect [non-linear response region]
3) high frequency region (higher than 5 Hz): low strain amplitude and short wave length [large effect of damping, and linear or non-linear response region]

In this study the reference deviation in the iterative calculation is fixed as 5 % for each frequency region. The continuity of equivalent strain $\gamma_f(\omega)$ along the frequency axis is still kept even the convergence judgement is separately performed in each frequency region. In case of response analysis in the following, the number of iterations in FDEL is in the range of 5 to 10 times which is similar to that of CVT.

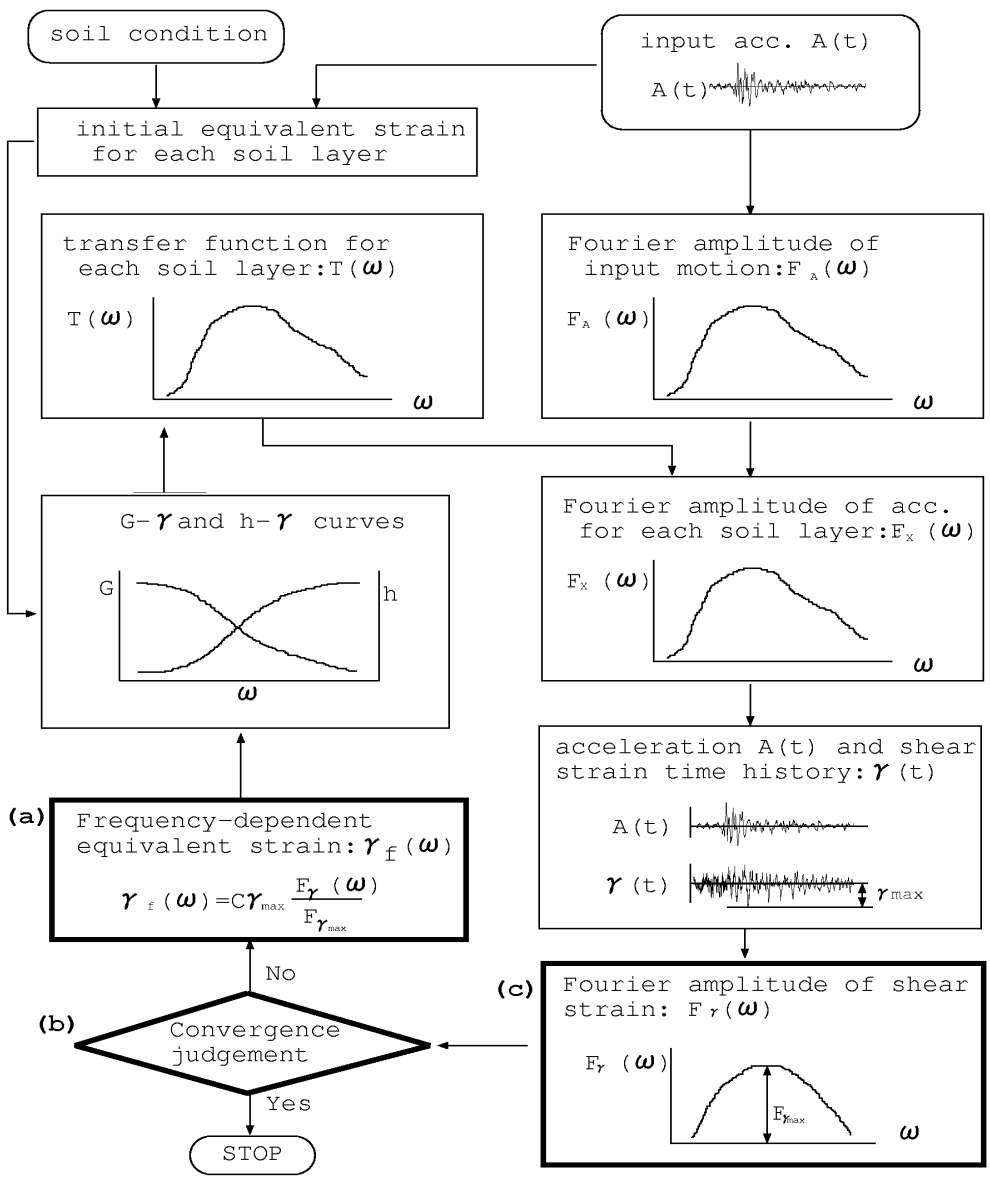

Figure 2. Flow-chart of response analysis in FDEL

Figure 2 shows flow-chart of the numerical calculation of FDEL. The three parts represented by thick solid line (a), (b), and (c) in the figure represent the characteristic parts of FDEL, which differ from CVT.

The equivalent strain is given according to the Fourier amplitude of strain time history in each soil layer [(a), (c)], and the convergence of iterative calculation is evaluated in each three frequency ranges [(b)].

EFFECTIVE STRESS BASED FEM (LIQCA)

Governing equations

The governing equations of for the coupling problems between soil skeleton and pore water were used based on a u-p formulation (Oka et al. [4]). The finite element method (FEM) has been usually used for the spatial discretization of the governing equations. In this study, however, the finite element method (FEM) was used for the spatial discretization of the equilibrium equation, while the finite difference method (FDM) was used for the spatial discretization of the pore water pressure in the continuity equation. The accuracy of the proposed numerical method was verified by Oka et al. [4] through a comparison of numerical results and analytical solutions for transient response of saturated porous solids.

The governing equations are formulated by the following assumptions; 1) the infinitesimal strain, 2) the smooth distribution of porosity in the soil, 3) the small relative acceleration of the fluid phase to that of the solid phase compared with the acceleration of the solid phase, 4) incompressible grain particles in the soil. The equilibrium equation for the mixture is derived as follows:

$$\rho \ddot{u}_i^s = \sigma_{ij,j} + \rho b_i \tag{7}$$

where ρ is the overall density, $\ddot{u}_i^s$ is the acceleration of the solid, σ_{ij} is the total stress tensor and b_i is the body force. The continuity equation is derived as follows:

$$\rho^f \ddot{\varepsilon}_{ii}^s - p_{,ii} - \frac{\gamma_w}{k}\dot{\varepsilon}_{ii}^s + \frac{n\gamma_w}{kK^f}\dot{p} = 0 \tag{8}$$

where ρ^f is the density of the fluid, p is the pore water pressure, γ_w is the unit weight of the fluid, k is the coefficient of permeability, ε_{ii}^s is the volumetric strain of the solid, n is porosity and K^f is the bulk modulus of the fluid.

Constitutive models

The constitutive equation used for sand is a cyclic elasto-plastic model (Oka et al. [5]) The constitutive equation is formulated by the following assumptions; 1) the infinitesimal strain, 2) the elasto-plastic theory, 3) the non-associated flow rule, 4) the concept of the overconsolidated boundary surface, 5) the non-linear kinematic hardening rule. The performance of the constitutive model was verified by Oka et al. [5]. The model succeeded in reproducing the experimental results well under various stress conditions, such as isotropic and anisotropic consolidated conditions, with and without the initial shear stress conditions, principal stress axis rotation, etc.

NUMERICAL SIMURATION

Determination of the index of liquefaction potential, P_L and P_{EL}

In the specifications for Highway Bridges [6], the earthquake motion is considered at the ground surface. On the other hand, in an equivalent linearized technique (SHAKE or FDEL), the maximum shear stress can be obtained for each ground layer. The shear stress ratio, L, is determined by the ratio between the maximum shear stress calculated and effective overburden pressure for each layer. The liquefaction resistance factor, F_L, is determined by the ratio between the dynamic shear strength ratio, R and L, as

$$F_L = R / L \tag{9}$$

The index of the liquefaction potential, P_L, is obtained by the following equation,

$$P_L = \int_0^{20} (1 - F_L)(10 - 0.5x)dx \tag{10}$$

where x is the depth (m) from the ground surface.

On the other hand, F_L cannot be determined directly with the result obtained by an effective stress based finite element analysis, LIQCA. In order to obtain the liquefaction resistance factor, we have proposed a liquefaction threshold, E_L, in terms of the excess pore water pressure ratio. We assume that the liquefaction occurs under the condition $E_{PR} > E_L$. In this study , the value of the liquefaction threshold, E_L, has been assumed to be 0.7 through a trial and error process. The liquefaction resistance factor based on LIQCA, F_{PR} is newly proposed and obtained based on excess pore water pressure ratio, E_{PR} and liquefaction threshold, E_L (see Figure 3).

$$F_{PR} = \begin{cases} \dfrac{E_{PR} - E_L}{1 - E_L} & (E_L < E_{PR}) \\ 0 & (0 < E_{PR} \le E_L) \end{cases} \tag{11}$$

Once we obtain F_{PR}, we can also calculate the index of the liquefaction potential, P_{EL} in place of P_L as,

$$P_{EL} = \int_0^{20} (1 - F_{PR})(10 - 0.5x)dx \tag{12}$$

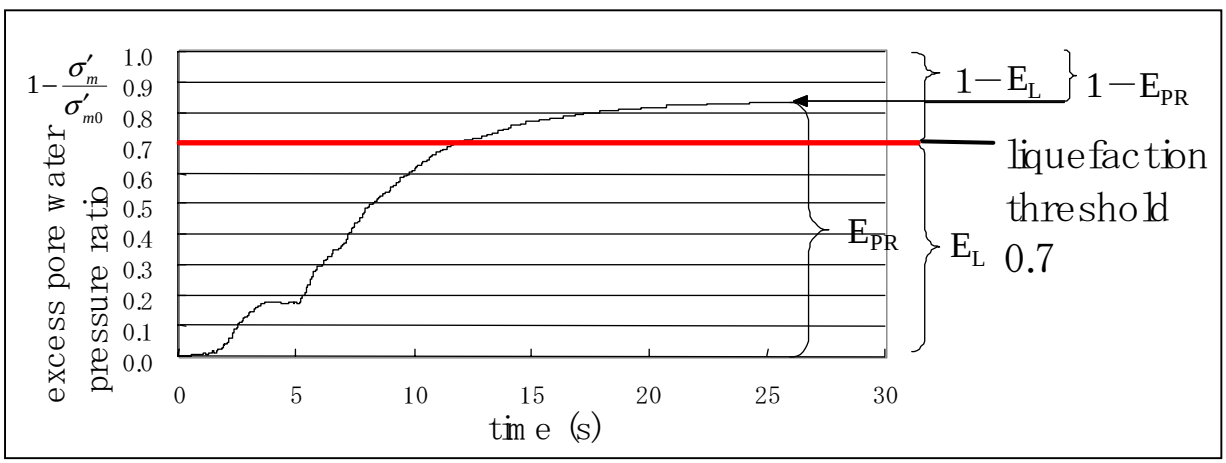

Figure 3. Liquefaction threshold, E_L and E_{PR}

Ground model for the analysis

In this study, three typical ground conditions are investigated. The distributions of SPT N-values and S-wave velocities at site A, B and C are shown in Figure 4.

1) Site A: The ground water table is at the ground surface. SPT N-value is very low from the ground surface down to G.L.-14 m. Several silty soil layers are sandwiched with very loose sandy layers.

2) Site B: The ground water table is at G.L.-2.1 m. The ground consists of sandy layer from the ground surface down to G.L.-18 m with relatively high SPT N-value. The soft silty soil layer exists between G.L.-18 m and G.L.-20 m.
3) Site C: The ground water table is at G.L.-3.5 m. The ground consists of reclaimed sandy layer with gravels from the ground surface down to G.L.-17 m. The SPT N-value for the reclaimed layer is less than 10.

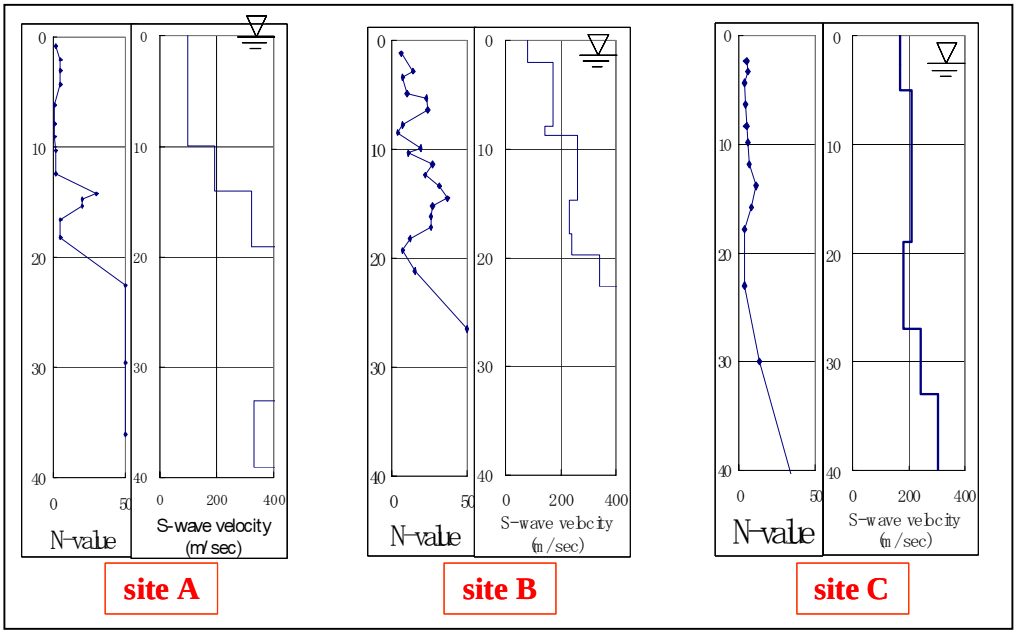

Figure 4. SPT N-value and S-wave velocity for three sites

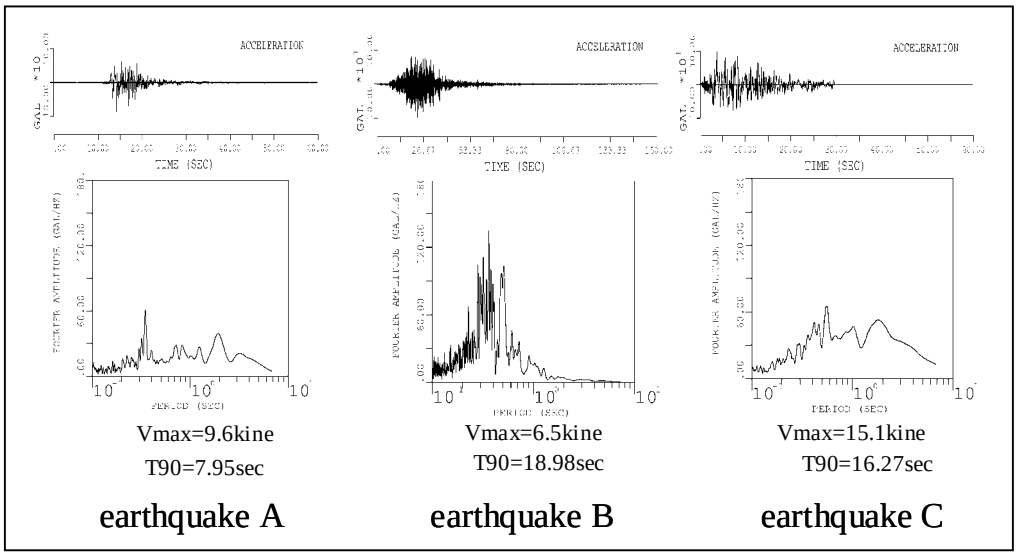

Figure 5. Input accelerations and Fourier spectra for three earthquakes

Input acceleration

Three input acceleration motions are prepared for the simulations. Figure 5 shows three input acceleration time histories with acceleration Fourier spectra. In this figure, the maximum accelerations are adjusted to 100 gal.

1) Input earthquake A: This acceleration time history was recorded at G.L.-83 m in the Port Island , Kobe city during the 1995 Hyogoken-Nambu Earthquake. The maximum velocity is the second largest among three input motions. The duration is 7.95 sec and the shortest among three input motions.
2) Input earthquake B: This acceleration time history was recorded at ground surface during the 1993 Kushiro-Oki Earthquake. The maximum velocity is the smallest and the duration is the longest among three input motions. A short period shaking is dominant.
3) Input earthquake C: This acceleration time history was recorded at ground surface during the 1999 Kocaeli (Turkey)-Earthquake. The maximum velocity is the largest and the duration is the second longest among three input motions. A relatively long period shaking is dominant.

NUMERICAL RESULT AND DISCUSSION

We first summarize the maximum input acceleration necessary to liquefy each soil layer. In Figure 6(a), (b) and (c), the distributions of the maximum input acceleration necessary to liquefy each soil layer are plotted. For site A, the maximum input accelerations are almost same except for silty soil layers regardless of type of numerical technique. For site B, larger accelerations are needed to liquefy sandy layers with relatively high SPT N-value for SHAKE and FDEL than LIQCA. It is found that equivalent linearized techniques show less conservative evaluation of the liquefaction potential than LIQCA.

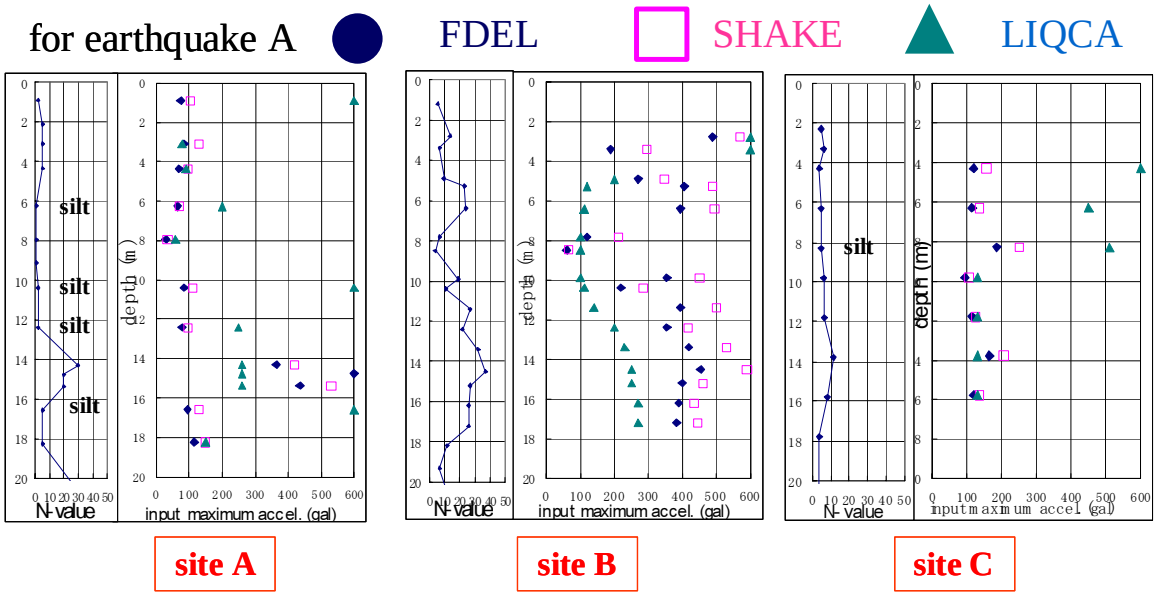

Figure 6(a). Maximum input acceleration necessary to liquefy each soil layer for earthquake A

For site C, once deeper sandy layers liquefy first, much larger accelerations are needed to liquefy upper sandy layers for LIQCA than SHAKE and FDEL. In equivalent linearized techniques, acceleration damping due to liquefaction cannot be taken into account. Therefore, larger shear stresses are transmitted through deeper liquefied layers for SHAKE and FDEL than LIQCA. It is found that equivalent linearized techniques show more conservative evaluation of the liquefaction potential than LIQCA if deeper layers liquefy first.

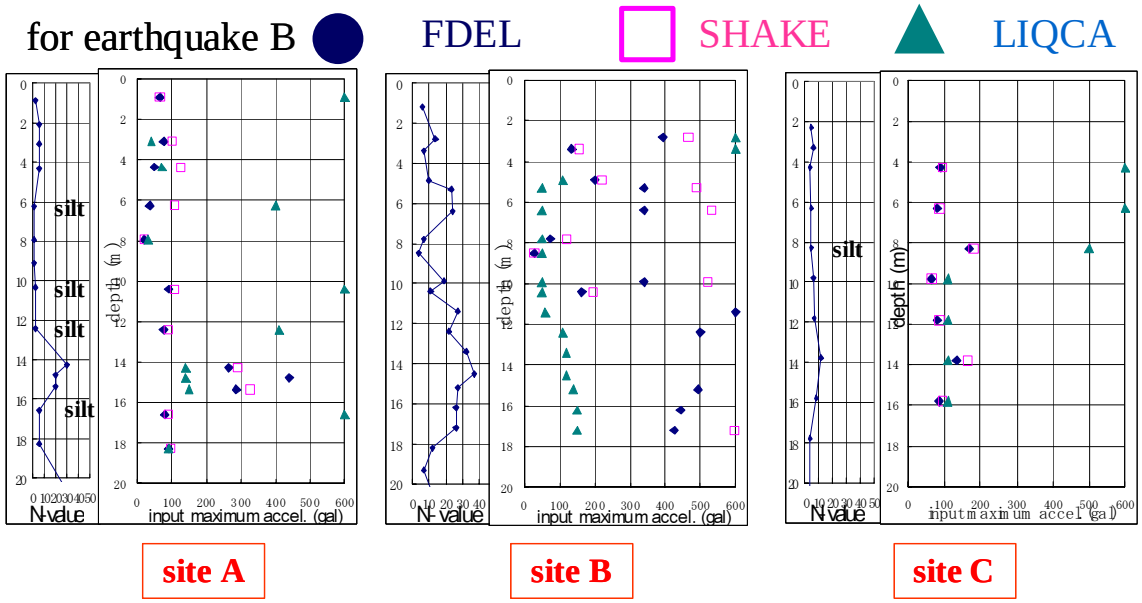

Figure 6(b). Maximum input acceleration necessary to liquefy each soil layer for earthquake B

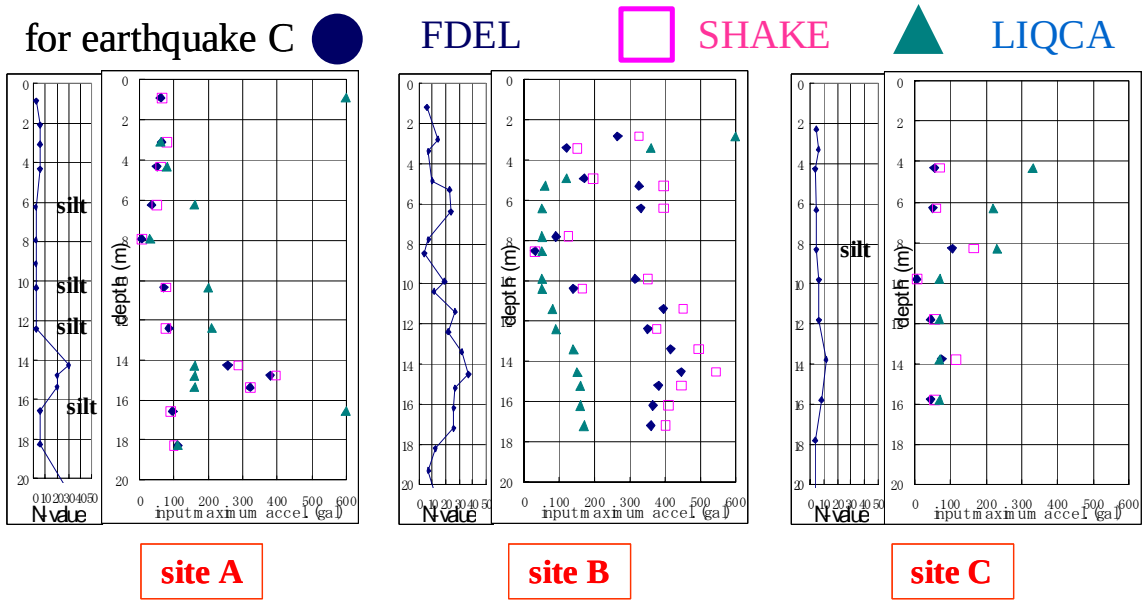

Figure 6(c). Maximum input acceleration necessary to liquefy each soil layer for earthquake C

Indexes of liquefaction potential, P_L and P_{EL} for each site are shown in Figure 7. For sites A and C, liquefaction potential predicted by SHAKE and FDEL are in good agreement with that by LIQCA. FDEL is found to give slightly higher liquefaction potential than SHAKE. This means that FEDL gives a slightly more conservative design for countermeasure against liquefaction than SHAKE. On the other hand, for site B with rather stiff deep ground, P_{EL}-value obtained by LIQCA is much higher than P_L-values obtained by SHAKE and FDEL especially for large input acceleration motions. This is because amplified shaking is transmitted from the base through rather stiff deeper layer into upper liquefiable layer in SHAKE and FDEL simulations.

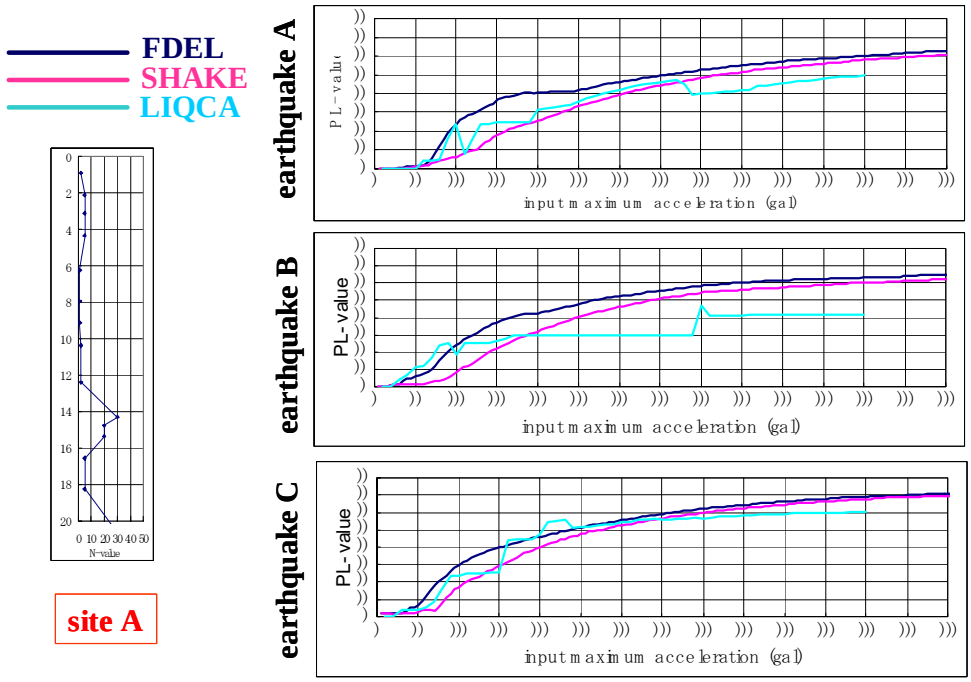

Figure 7(a). Index of liquefaction potential with respect to input maximum acceleration for site A

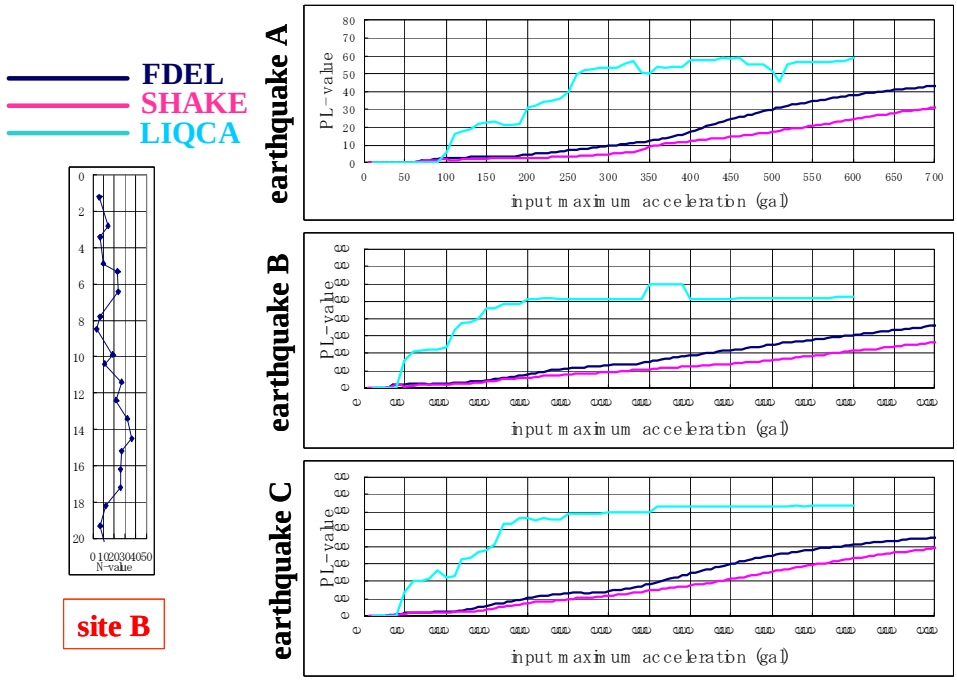

Figure 7(b). Index of liquefaction potential with respect to input maximum acceleration for site B

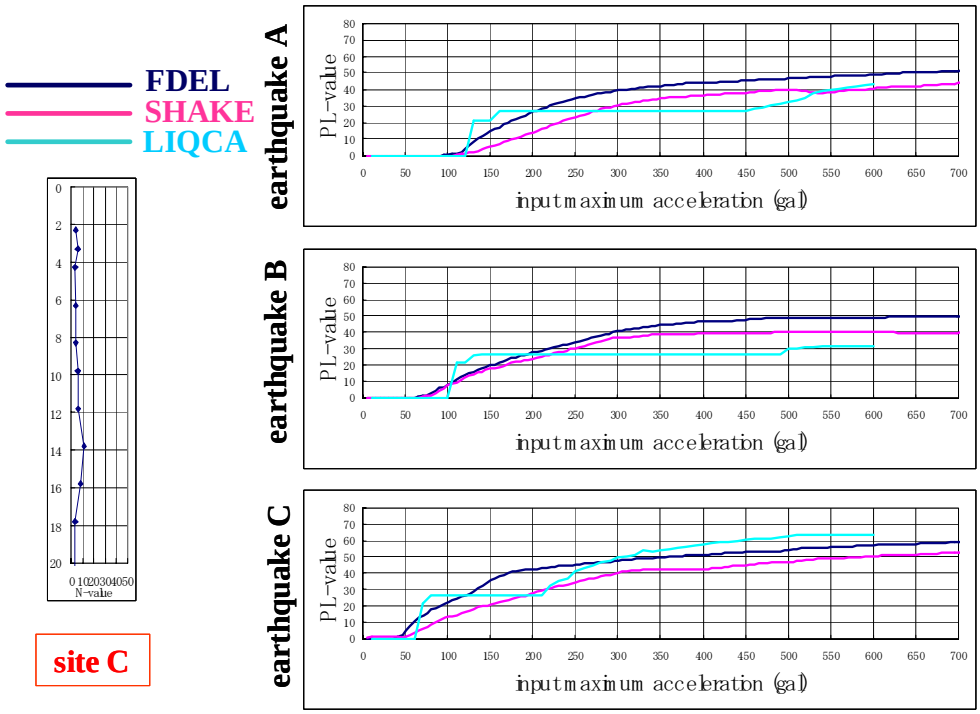

Figure 7(c). Index of liquefaction potential with respect to input maximum acceleration for site C

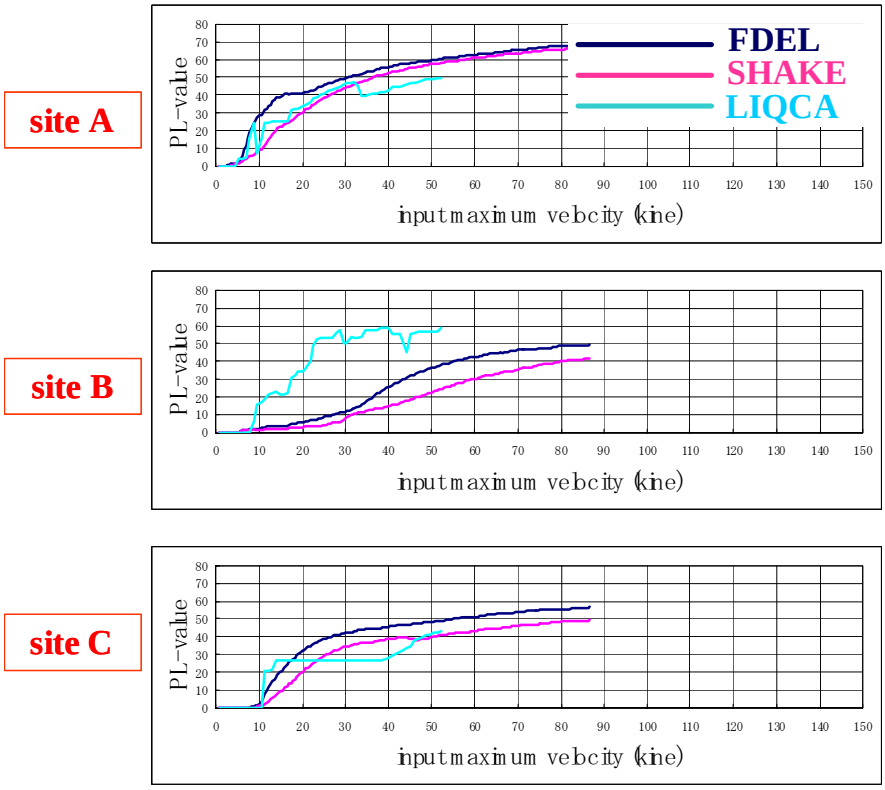

Figure 8(a). Index of liquefaction potential with respect to input maximum velocity for earthquake A

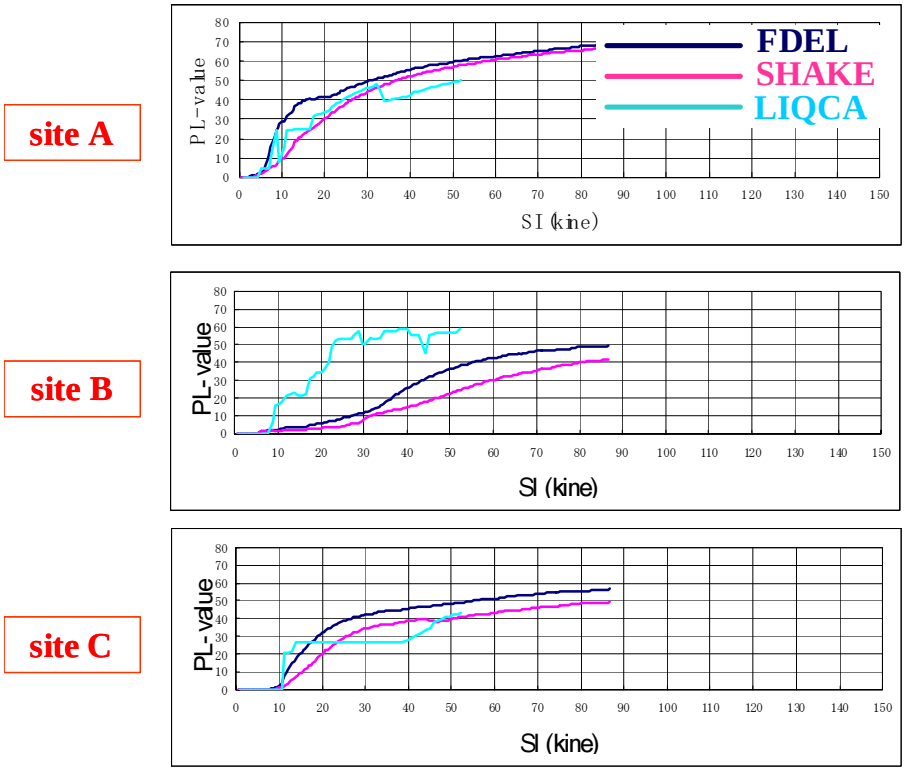

Figure 8(b). Index of liquefaction potential with respect to SI-value for earthquake A

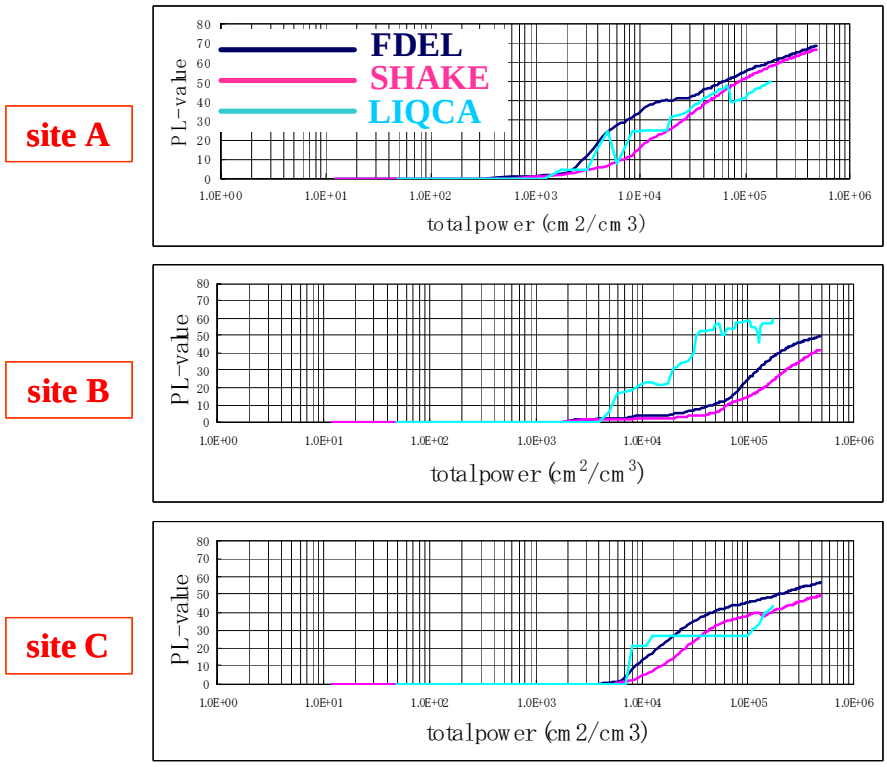

Figure 8(c). Index of liquefaction potential with respect to total power for earthquake A

Indexes of liquefaction potential for input earthquake A are plotted in Figure 8 with respect to input maximum velocity, SI-value and total power, respectively. Except for site B, equivalent linearized techniques predict liquefaction potential very well as in the case of LIQCA.

The index of liquefaction potential builds up at certain magnitude of input acceleration, velocity, SI-value and total power, respectively. Figure 9 summarizes the magnitude of acceleration, velocity, SI-value and total power at which the index of liquefaction potential first builds up for three sites under three different earthquake motions. From this figure, it is found that larger the velocity and longer the duration are, the ground can be liquefied faster. On the other hand, there is no difference among three earthquake motions if we introduce the value of total power at base as the trigger of liquefaction.

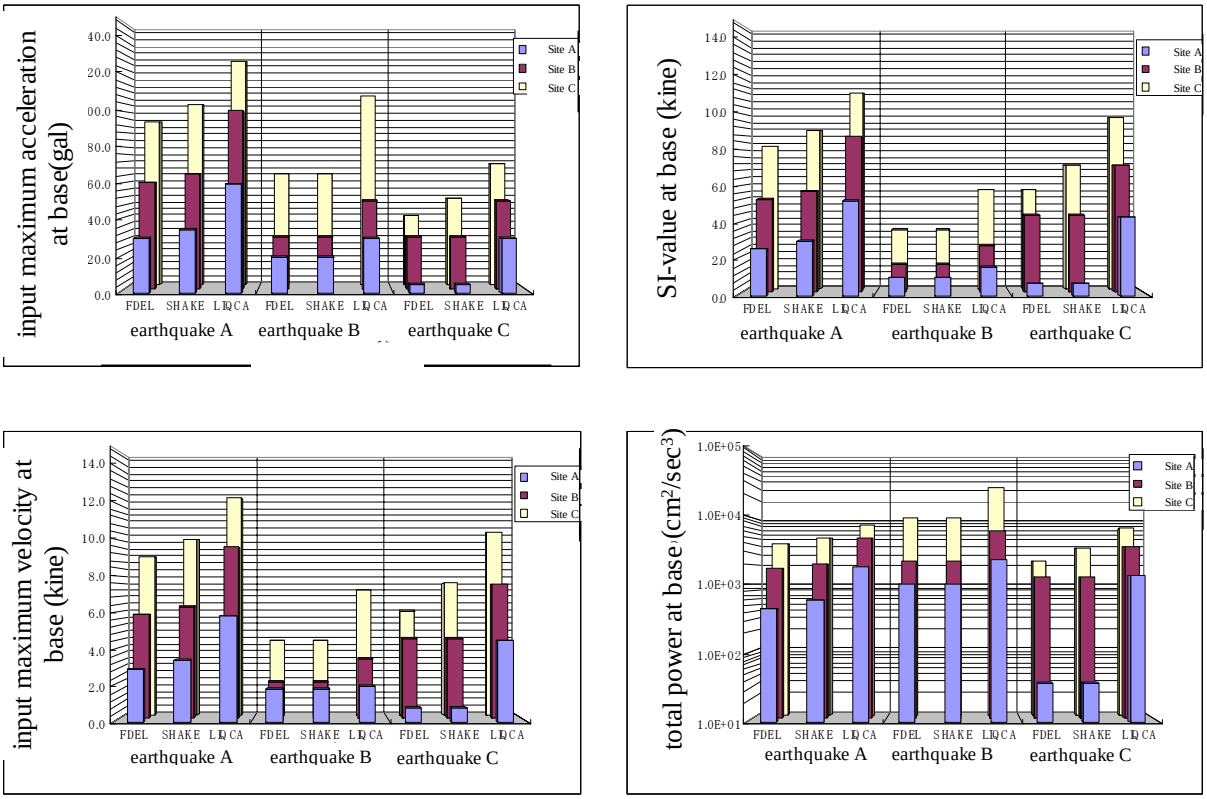

Figure 9. Magnitude of acceleration, velocity, SI-value and total power at which the index of liquefaction potential first builds up for three sites under three different earthquake motions

CONCLUSIONS

In the present paper, a conventional equivalent linearized technique (SHAKE), a frequency-dependent equivalent linearized technique (FDEL) and an effective stress based FEM technique (LIQCA) were used to evaluate the liquefaction potential for three typical ground under different input motions. In the finite element analysis, the liquefaction resistance factor was newly proposed by introducing the liquefaction threshold. The liquefaction potentials obtained by SHAKE and FDEL were carefully compared with those obtained from the effective stress based FEM.

The obtained conclusions can be summarized as follows:

a) For loose sandy layers, liquefaction potential predicted by SHAKE and FDEL are in good agreement with that by LIQCA. On the other hand, for rather stiff ground, liquefaction potential obtained by LIQCA is much higher than that obtained by SHAKE and FDEL for large input acceleration motions. This is because amplified shaking is transmitted from the base through rather stiff deeper layer into upper liquefiable layer
b) A frequency-dependent equivalent linearized technique (FDEL) predicts slightly higher liquefaction potential than a conventional equivalent linearized technique (SHAKE). Larger the earthquake shaking is, the deference between FDEL and SHAKE becomes larger.
c) It is found that larger the velocity and longer the duration are, the ground can be liquefied faster.
d) If we introduce the value of total power at base as the trigger of liquefaction, there is no difference among three input earthquake motions considered in this study.

REFERENCES

1. Schnabel, P. B., Lysmer, J. and Seed, H. B. “SHAKE a computer program for earthquake response analysis of horizontally layered sites.” Proc. of EERC, 1972: 72-12.
2. Sugito, M. Goda, H. and Masuda, T. “Frequency-dependent equi-linearized technique for seismic response analysis of multi-layered ground.” Proc. of JSCE, 1994: No.493/III-27: 49-58 (in Japanese).
3. Hardin, B. O. and V. P. Drnevich. “Shear modulus and damping in soils.” Proc. ASCE, 1972: 98(SM6).
4. Oka, F., Yashima, A., Shibata, T., Kato, M., and Uzuoka, R. “FEM-FDM coupled liquefaction analysis of a porous soil using an elasto-plastic model”, Applied Scientific Research, 1994: 52: 209-245.
5. Oka, F., Yashima, A., Tateishi, A., Taguchi, Y. and Yamashita, S. “A cyclic elasto-plastic constitutive model for sand considering a plastic-strain dependence of the shear modulus”, Geotechnique, 1999: No.5(49): 661-680.